

Ridge waveguide DBR laser with nonabsorbing grating and transparent integrated waveguide

D. Hofstetter, H.P. Zappe and J.E. Epler

Indexing terms: Distributed Bragg reflector lasers, Semiconductor quantum wells

A ridge waveguide GaAs/AlGaAs DBR laser with a nonabsorbing grating section and a monolithically integrated transparent waveguide has been fabricated by the use of vacancy-enhanced quantum well disordering (VED). This technique allows the definition of absorbing and transparent regions, and requires only a single growth step. No VED-enhanced degradation of the laser quality was noted. The optical output power was 5 mW from both the cleaved facet and the grating reflector, threshold currents were 25 mA and the slope efficiencies were 0.2W/A.

Introduction: Monolithic photonic integrated circuits (PICs) often require coherent light sources without cleaved laser facets. Distributed Bragg reflector (DBR) lasers are ideally suited to this application. Furthermore, a method is needed to produce absorbing and nonabsorbing regions on the same substrate without degrading laser performance. Pumped laser sections and photodetectors need to absorb at the operating wavelength, whereas the waveguides and the grating section of the DBR laser must be transparent. DBR lasers with a transparent grating section fabricated by vacancy-enhanced disordering (VED) [1] and DBR lasers evanescently coupled with a transparent waveguide [2] have been reported. The first of these approaches demonstrated that the VED process can shift the energy bandgap, albeit at the cost of a very high laser threshold current, whereas the latter required extended regrowth technology.

In this Letter, we demonstrate the use of the VED process to fabricate a low threshold DBR laser with a nonabsorbing grating section, monolithically integrated with a 700 μ m long transparent waveguide. The device demonstrates the utility of postgrowth processing for achieving spatially-defined transparency in a PIC. VED selectively alters the shape of the quantum well (QW) in the active region, using lift-off patterned SrF₂ and SiO₂ surface dielectrics to define the transparent and absorbing regions and a high temperature rapid thermal anneal to accomplish disordering [3].

Device fabrication: An MOVPE layer structure grown on an *n*-type, Si-doped, (10¹⁸cm⁻³) GaAs substrate was used to fabricate the device. An undoped 165 nm thick Al_{0.3}Ga_{0.7}As core containing a single 7 nm wide GaAs quantum well was grown between a 1.1 μ m thick Al_{0.3}Ga_{0.7}As lower cladding layer (*n*-doped 1.5 \times 10¹⁸cm⁻³ Si) and a 0.8 μ m thick Al_{0.3}Ga_{0.7}As upper cladding layer (*p*-doped 10¹⁸cm⁻³ Mg). The upper cladding was covered with a 100 nm thick highly *p*-doped (8 \times 10¹⁹cm⁻³ Zn) GaAs cap layer. The VED process started with a 200 nm thick e-beam evaporated SiO₂ layer, patterned by standard photolithography and reactive ion etching (RIE) in a CF₄ plasma. Using a selfaligned process, a 250 nm thick SrF₂ layer was subsequently evaporated, and removed from the underlying SiO₂ by liftoff. The final wafer surface was nearly planar and completely covered with either SiO₂ or SrF₂. The selective bandgap-shift was then accomplished using a rapid thermal anneal in an N₂ ambient at 960°C for 24s.

During thermal annealing, the group-III vacancies generated under the SiO₂-capped regions diffuse through the upper cladding into the waveguide core. These vacancies promote intermixing of the Ga in the GaAs QW and the Al of the adjacent Al_{0.3}Ga_{0.7}As waveguide core, increasing the effective Al content of the QW.

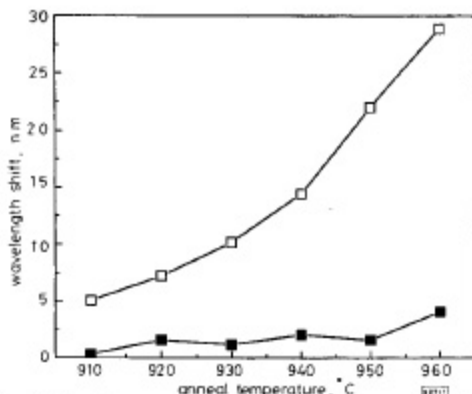


Fig. 1 Photoluminescence wavelength shift of SiO₂-capped and SrF₂-capped material after 30s rapid thermal anneal at various temperatures

□— SiO₂ cap
■— SrF₂ cap

The resulting larger bandgap blue-shifts the photoluminescence (PL) spectrum and thus the lasing wavelength. SrF₂, on the other hand, suppresses the generation of these group-III vacancies and no blue shift occurs during thermal annealing. As seen in Fig. 1, the amount of blue shift under the SiO₂ cap can be varied between 5 and 28 nm with the anneal temperature, while on the same wafer under the same anneal conditions, the blue shift under the SrF₂ cap is only 1–5 nm. The anneal time is held constant at 30s in both cases. During RTA, a GaAs proximity cap prevents surface damage of the sample due to As outdiffusion [4].

After RTA, SrF₂ and SiO₂ were removed with diluted HCl (HCl/H₂O 1:9, 20s) and by RIE in CF₄, respectively. Lasers were then fabricated by dry etching ridge waveguides, deposition of 250 nm Si₃N₄ as an electrical isolation layer and Ti/Pt/Au *p*-contact metallisation. The holographically-defined third-order grating ($\Lambda = 380$ nm) was fabricated in a grating recess as described in [5]. DBR lasers with ridge widths of 2.3 and 4 μ m, a constant pumped length of 500 μ m and six different grating section lengths (50 to 150 μ m) were made and comparatively characterised. The lasers and gratings were integrated with a 700 μ m long transparent waveguide.

Results: As seen in Fig. 2, DBR laser threshold currents were typically 25 mA on devices with 4 μ m stripe width and a 500 μ m pumped length, corresponding to a threshold current density of 1.25 kA/cm². The ripples in the L-I curve for optical output from the cleaved facet are reproducible and without hysteresis when increasing and decreasing the injection current. They indicate that the laser has to optimise its internal stored energy under changing phase conditions due to carrier and temperature induced refractive index changes. The ripples in the L-I curve were less pronounced for emission from the grating side of the laser than from the cleaved facet. We believe that this results from a trade-off between the grating transmission and the internal laser stored energy. A decrease in grating reflectivity induces a simultaneous decrease of the internal power and since the output power is the product of internal power and mirror transmission, nearly constant laser output power is expected.

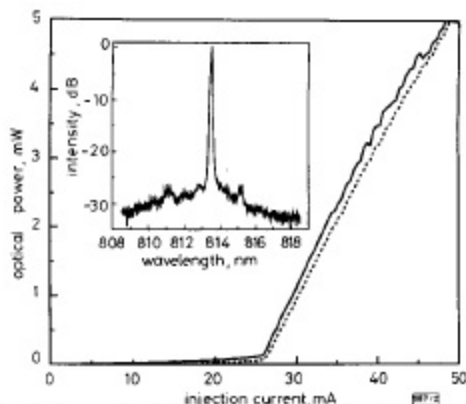


Fig. 2 L-I curves of emission from the cleaved facet and the grating plus the transparent waveguide

— P_{opt} (cleaved facet)
 - - - P_{opt} (grating side facet)
 Inset: optical spectrum

The optical output power was 5 mW from both the cleaved facet and the grating side of the DBR laser at $I = 2I_{th}$ and the slope efficiencies were 0.21 W/A at the cleaved facet and 0.19 W/A at the grating. This balance is due to the low grating reflectivity (<30%) and the transparency of the waveguide. The optical emission spectrum, shown in the inset of Fig. 2, shows a primary emission peak at $\lambda = 814$ nm and an SMSR of 25 dB. No mode hops were seen as the temperature was varied from 7 to 25°C; the temperature tuning coefficient was 0.05 nm/°C.

A comparison of Fabry-Perot lasers fabricated from the annealed but unshifted (SrF₂ capped) and as-grown (unannealed) material provided a further demonstration that high-quality lasers can be fabricated using VED. The former devices operated with a threshold current of 14 mA ($J_{th} = 700$ A/cm²), slope efficiency of 0.36 W/A per facet at an emission wavelength of $\lambda = 825$ nm with SMSR = 20 dB. In as-grown material, the same laser structures yielded a threshold current of 12 mA ($J_{th} = 600$ A/cm²) and a slope efficiency of 0.52 W/A per facet at an emission wavelength of $\lambda = 827$ nm with SMSR = 20 dB, demonstrating that devices produced in high temperature annealed material are of comparable quality to those produced in as-grown material. In contrast to results published in [6], we could not see any dopant diffusion or a drift of the pn-junction by inspecting the stained facet in the scanning electron microscope. These data also helped to explain the somewhat high threshold current density of the DBR lasers, owing to the mismatch between the Bragg peak of the grating (814 nm) and the laser gain peak (825 nm).

Conclusions: Low threshold DBR lasers monolithically integrated with a transparent waveguide have been fabricated using selective vacancy-enhanced disordering. The performance of the laser was not adversely affected by the high temperature anneal required for VED, demonstrating the utility of this process for PIC fabrication.

Acknowledgments: The authors are grateful to M. Moser and H.P. Schweizer for crystal growth, P. Riel, A. Vonlanthen and D. Jeggle for processing assistance, J. Stöchtig for helpful discussions and H.W. Lehmann, M.T. Gale and R. Dändliker (IMT, University of Neuchâtel) for their generous support.

D. Hofstetter, H.P. Zappe and J.E. Epler (Paul Scherrer Institut Zürich, Badenerstrasse 569, CH-8048 Zürich, Switzerland)

References

- AYLING, S.G., BEAUVAIS, J., and MARSH, J.H.: 'A DBR laser using dielectric cap disordering and strontium fluoride masking', *Proc. ECIO*, 1993, **1993**, pp. 7-10-7-11
- DEBI, R.J., DOLDISSEN, W., HAWKINS, R.J., BHAT, R., SOOLE, J.B.D., SCHIAVONE, L.M., SETO, M., ANDREADAKIS, N., SILBERBERG, V., and KOZA, M.A.: 'Efficient vertical coupling of photodiodes to InGaAsP rib waveguides', *Appl. Phys. Lett.*, 1991, **71**, pp. 2749-2751
- BEAUVAIS, J., MARSH, J.H., KEAN, A.H., BRYCE, A.C., and BUTTON, C.: 'Suppression of bandgap shifts in GaAs/AlGaAs quantum wells using strontium fluoride caps', *Electron. Lett.*, 1992, **28**, pp. 1670-1672
- GUIDO, L.J., HOLONYAK, N., HSIEH, K.C., KALISKI, R.W., PLANO, W.E., BURNHAM, R.D., THORNTON, R.L., EPLER, J.E., and PAOLI, T.L.: 'Effects of dielectric encapsulation and As overpressure on Al-Ga interdiffusion in Al_{0.5}Ga_{0.5}As/GaAs quantum well heterostructures', *J. Appl. Phys.*, 1987, **61**, pp. 1372-1379
- HOFSTETTER, D., ZAPPE, H.P., EPLER, J.E., and SÖCHTIG, J.: 'Single-growth-step GaAs/AlGaAs distributed Bragg-reflector lasers with holographically-defined recessed gratings', *Electron. Lett.*, 1994, **30**, pp. 1858-1859
- AYLING, S.G., BRYCE, A.C., GONTO, I., MARSH, J.H., and ROBERTS, J.S.: 'A comparison of carbon and zinc doping in GaAs/AlGaAs lasers band-gap tuned by impurity-free vacancy disordering', *Semicond. Sci. Technol.*, 1994, **9**, pp. 2149-2151